262 *Macromolecules* **2010**, *43*, 262–270
DOI: 10.1021/ma901526j

Macromolecules
ARTICLE

PAA-*g*-PPO Amphiphilic Graft Copolymer: Synthesis and Diverse Micellar Morphologies

Yaogong Li,[†] Yaqin Zhang,[†] Dong Yang,[‡] Yongjun Li,[†] Jianhua Hu,*[,‡] Chun Feng,[†] Sujuan Zhai,[†] Guolin Lu,[†] and Xiaoyu Huang*[,†]

[†]*Key Laboratory of Organofluorine Chemistry and Laboratory of Polymer Materials, Shanghai Institute of Organic Chemistry, Chinese Academy of Sciences, 345 Lingling Road, Shanghai 200032, P. R. China, and* [‡]*Key Laboratory of Molecular Engineering of Polymers* (*Ministry of Education*), *Laboratory of Advanced Materials and Department of Macromolecular Science, Fudan University, 220 Handan Road, Shanghai 200433, P. R. China*

Received July 13, 2009; Revised Manuscript Received September 3, 2009

ABSTRACT: A series of well-defined amphiphilic graft copolymers consisting of hydrophilic poly(acrylic acid) backbone and hydrophobic poly(propylene oxide) side chains were synthesized by sequential reversible addition−fragmentation chain transfer (RAFT) polymerization and atom transfer nitroxide radical coupling (ATNRC) chemistry followed by selective hydrolysis of poly(*tert*-butyl acrylate) backbone. A new Br- containing acrylate monomer, *tert*-butyl 2-((2-bromopropanoyloxy)methyl) acrylate, was first prepared, and it can be polymerized via RAFT in a controlled way to obtain a well-defined homopolymer with narrow molecular weight distribution ($M_w/M_n = 1.06$). Grafting-onto strategy was employed to synthesize P*t*BA-*g*-PPO well-defined graft copolymers with narrow molecular weight distributions ($M_w/M_n = 1.05-1.23$) via ATNRC reaction between Br-containing P*t*BA-based backbone and poly(propylene oxide) with 2,2,6,6-tetramethylpiperidine-1-oxyl (TEMPO) end group using CuBr/PMDETA or Cu/PMDETA as catalytic system. The final PAA-*g*-PPO amphiphilic graft copolymers were obtained by the selective acidic hydrolysis of P*t*BA backbone in acidic environment without affecting the side chains. The critical micelle concentrations in aqueous media were determined by a fluorescence probe technique. Diverse micellar morphologies were formed with varying the content of hydrophobic PPO segment.

Introduction

Poly(propylene oxide) (PPO) is a kind of nonionic polymer, and it is soluble in most common organic solvents whereas hardly soluble in water. PPO can be applied in many fields such as lubricants, surfactants, hydraulic pressure liquid, and so on.[1−3] In particular, PPO segment can be used to modulate the properties of polymeric solution by its incorporation into a macromolecule.[4] Many synthetic pathways are available for the preparation of well-defined block copolymers comprising PPO block.[5,6] Each segment can be prepared independently and connected by the postpolymerization coupling of functional end groups. Moreover, PPO homopolymer prepared by anionic polymerization contains one or two hydroxyl end functionalities, and this kind of commercially available functional PPO homopolymer is in favor of almost unlimited chemical modification. PPO-based block copolymers (PEO was usually selected as another block)[5−19] have been extensively studied due to their convenient syntheses, and only a few examples touched on PPO-based graft copolymers.[20−28] Most of these graft copolymers were synthesized from PPO-based macromonomers containing (meth)acrylate end groups using living or traditional radical polymerization, and ester linkages were employed to connect PPO side chains with the hydrophobic backbone in these "graft" copolymers, implying PPO segments would be detached after the hydrolysis of ester connections.[20−23] PPO-based graft copolymers can also be obtained via other types of PPO-based macromonomers by the condensation polymerization or catalyzed coupling polymerization.[24,25] Moreover, nucleophilic substitution reactions[26,27] were also applied to synthesize the graft copolymers containing PPO side chains, whose backbone and side chains were prepared independently; however, the grafting densities of these graft copolymers were not clear[26] or very low (60/1230 = 4.88%),[27] and they possessed broad molecular weight distributions,[26,27] this indicating that these graft copolymers might not be well-defined. The pendant hydroxyls of ethylene−vinyl alcohol copolymer were also employed to initiate anionic graft polymerization of propylene oxide to afford the densely grafted polymers containing PPO side chains.[28] However, none has reported the well-defined amphiphilic graft copolymer bearing hydrophilic backbone and hydrophobic PPO side chains.

Generally, polymer chemists employed three strategies including grafting-through, grafting-from, and grafting-onto to synthesize the graft copolymer.[29] Graft copolymers can be obtained via the polymerization of macromonomers using the grafting-through strategy, the resulting graft copolymers via the conventional radical polymerization possessed a broad chain-length distribution,[30] and living polymerization yielded well-defined graft copolymers with low molecular weights.[31] The grafting-from approach utilized the pendant initiation groups on the backbone to initiate the polymerization (generally employing living radical polymerization including atom transfer radical polymerization (ATRP),[32−34] reversible addition−fragmentation chain transfer (RAFT) polymerization,[35,36] and single-electron-transfer living radical polymerization (SET-LRP)[37,38]) of another monomer to form the side chains.[39,40] The grafting-onto

*To whom correspondence should be addressed: e-mail hujh@fudan.edu.cn, Tel +86- 21-55665280, Fax +86-21-65640293 (J.H.); e-mail xyhuang@mail.sioc.ac.cn, Tel +86-21-54925310, Fax +86-21-64166128 (X.H.).

 Published on Web 11/04/2009

method is to attach the side chains onto the backbone by a coupling reaction.[41] In this situation, both the backbone and side chains can be prepared and characterized independently, so it is easy to synthesize the graft copolymers with certain structures. Since propylene oxide cannot be polymerized by living radical polymerization, it is impossible to employ the grafting-from strategy to obtain the graft copolymers with PPO side chains. Thus, the grafting-onto strategy is a suitable approach to synthesize well-defined amphiphilic graft copolymers containing hydrophobic PPO side chains due to the commercial availability of well-defined PPO homopolymer possessing hydroxyl end functionalities. However, this technique requires high coupling efficiency between the backbone and the side chains.[41]

As a highly efficient coupling reaction, click chemistry[42] has been extensively applied for the construction of well-defined (functional) polymer architectures;[43−46] however, special care must be taken due to the instability of azide compounds.[47] Recently, Huang and co-workers reported a new coupling reaction called atom transfer nitroxide radical coupling (ATNRC) chemistry,[47−51] which was realized by mixing a TEMPO-containing polymer with another Br-containing polymer in the presence of CuBr/PMDETA catalytic system. The coupling efficiency of ATNRC was as high as 90%,[48,49] which is similar to that of click chemistry. Thus, ATNRC can serve as a relatively convenient and safe way with "click-like" efficiency to synthesize the graft copolymers with certain structures using the grafting-onto strategy.

In this work, we reported the synthesis of poly(acrylic acid)-*g*-poly(propylene oxide) (PAA-*g*-PPO) well-defined amphiphilic graft copolymer, whose backbone and side chains were both with certain and defined structures (Scheme 1). A new acrylic monomer, *tert*-butyl 2-((2-bromopropanoyloxy)methyl)acrylate (*t*BBPMA), was first prepared, and it was homopolymerized via RAFT to form well-defined Br-containing poly(*tert*-butyl acrylate)-based backbone. Next, well-defined poly(*tert*-butyl acrylate)-*g*-poly(propylene oxide) (P*t*BA-*g*-PPO) graft copolymers with narrow molecular weight distributions were synthesized via ATNRC between P*t*BA-based backbone and TEMPO-containing PPO side chains (PPO-TEMPO) catalyzed by CuBr/PMDETA or Cu/PMDETA. The final amphiphilic graft copolymers were obtained by the selective acidic hydrolysis of P*t*BA backbone, and they can form diverse micellar morphologies in aqueous media.

Experimental Section

Materials. *tert*-Butyl acrylate (*t*BA, Aldrich, 98%) was washed with 5% aqueous NaOH solution to remove the inhibitor, then washed with water, dried over $CaCl_2$, and distilled twice from CaH_2 under reduced pressure prior to use. CuBr (Aldrich, 98%) was purified by stirring overnight over CH_3CO_2H at room temperature, followed by washing the solid with ethanol, diethyl ether, and acetone prior to drying at 40 °C under vacuum for 1 day. Pyrene (Aldrich, 98%) was purified by recrystallization in ethanol for three times. 2,2′-Azobis(isobutyronitrile) (AIBN, Aldrich, 98%) was recrystallized from anhydrous ethanol. Triethylamine (TEA, Aldrich, 99.5%) was dried over KOH and distilled over CaH_2 under N_2 prior to use. Tetrahydrofuran (THF, Aldrich, 99%), dichloromethane (Aldrich, 99.5%), chloroform (Aldrich, 99%), and toluene (Aldrich, 99.8%) were dried over CaH_2 and distilled from sodium and benzophenone under N_2 prior to use. Cumyl

Scheme 1. Synthesis of PAA-*g*-PPO Well-Defined Amphiphilic Graft Copolymer

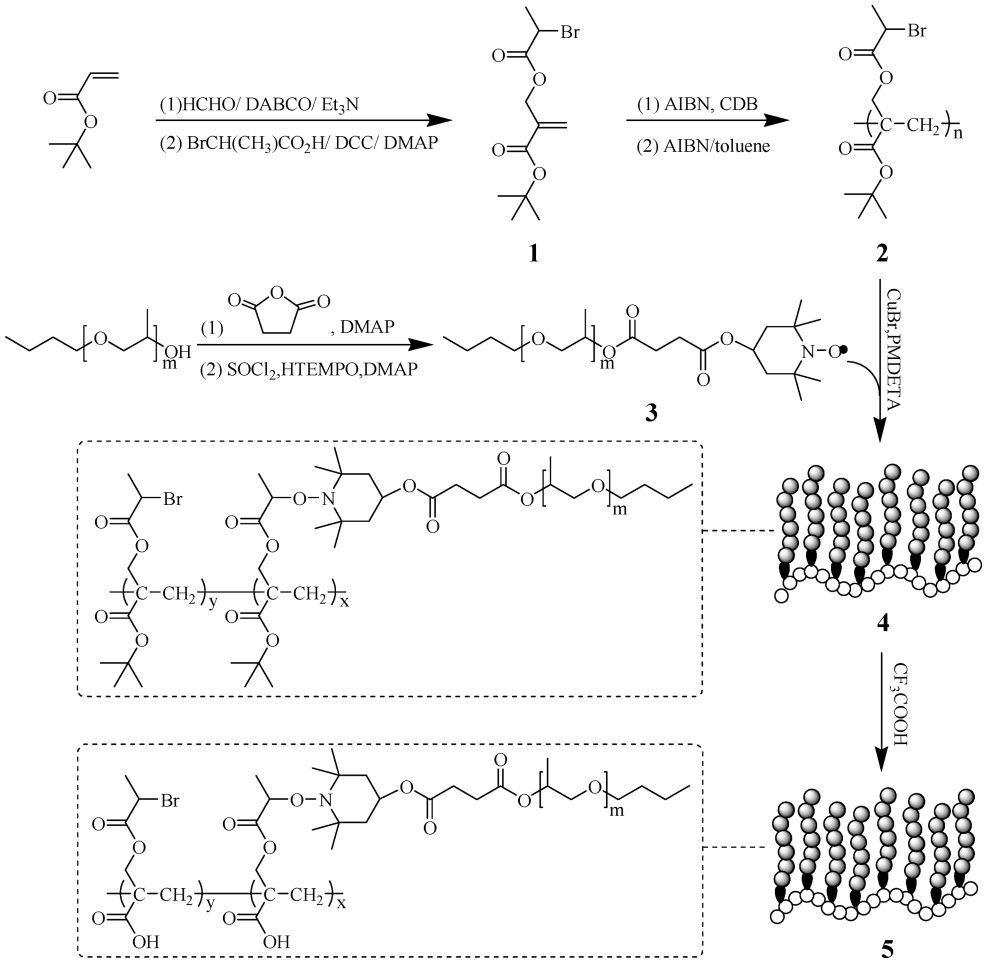

dithiobenzoate (CDB) was synthesized according to previous literature.[52] 2-Bromopropionic acid (Aldrich, 99%), copper powder (Aldrich, 99%), 4-hydroxy-2,2,6,6-tetramethylpiperidine-1-oxyl (HTEMPO, Aldrich, 97%), formalin (Aldrich, 38 wt %), poly(propylene oxide) monobutyl ether (PPO-OH, M_n = 1000 and 2500, Aldrich), 1,4-diazabicyclo[2.2.2]octane (DABCO, Aldrich, 98%), *N,N′*-dicyclohexylcarbodiimide (DCC, Aldrich, 99%), 4-di(methylamino)pyridine (DMAP, Aldrich, 99%), *N,N,N′,N′,N″*-pentamethyldiethylenetriamine (PMDETA, Aldrich, 99%), thionyl chloride (Aldrich, 99%), succinic anhydride (Aldrich, 99%), and trifluoroacetic acid (TFA, Aldrich, 99%) were used as received.

Measurements. FT-IR spectra were recorded on a Nicolet AVATAR-360 FT-IR spectrophotometer with a resolution of 4 cm^{-1}. All ^1H NMR (500 MHz) and ^{13}C NMR (125 MHz) analyses were performed on a Bruker Avance 500 spectrometer in $CDCl_3$, except that ^1H NMR spectrum of PPO-TEMPO was measured in CD_3OD in the presence of stoichiometric $HCOONH_4$ and Pd/C.[48] TMS (^1H NMR) and $CDCl_3$ (^{13}C NMR) were used as internal standards. Elemental analysis was carried out on a Carlo-Erba1106 system. Bromine content was determined by the titrations with $Hg(NO_3)_2$. ESI-MS was measured by an Agilent LC/MSD SL system, and MALDI-TOF-MS was measured by an Applied Biosystems Voyager DE-STR spectrometer. Relative molecular weights and molecular weight distributions were measured by conventional gel permeation chromatography (GPC) system equipped with a Waters 1515 isocratic HPLC pump, a Waters 2414 refractive index detector, and a set of Waters Styragel columns (HR3, HR4, and HR5, 7.8 × 300 mm). GPC measurements were carried out at 35 °C using THF as eluent with a flow rate of 1.0 mL/min. The system was calibrated with linear polystyrene standards. Steady-state fluorescent spectra were recorded on a Hitachi F-4500 spectrofluorometer with the bandwidths of 10 nm for excitation and 2.5 nm for emission, where λ_{ex} = 339 nm. Transmission electron microscope (TEM) images were obtained by a JEOL JEM-1230 instrument operated at 80 kV.

Synthesis of *tert*-Butyl 2-((2-Bromopropanoyloxy)methyl)-acrylate. Acrylic monomer **1** was synthesized in two steps using commercially available *tert*-butyl acrylate, formalin, and 2-bromopropionic acid as starting materials. First, *tert*-butyl acrylate reacted with formalin to give an intermediate of *tert*-butyl (2-hydroxymethyl)acrylate with a yield of 77.0%. Next, the desired acrylic monomer **1** was obtained via the reaction between the intermediate and 2-bromopropionic acid at room temperature with a yield of 94.4%. ESI-MS (*m*/*z*): found $(M - 56)^+$: 237. Anal. Calcd for $C_{11}H_{17}O_4Br$: C, 45.05%; H, 5.80%; Br, 27.30%. Found: C, 45.37%; H, 5.58%; Br, 27.20%. FT-IR: ν (cm^{-1}): 2979, 2934, 1748, 1720, 1643, 1448, 1394, 1369, 1146, 1063, 848, 816, 761, 515. ^1H NMR: δ (ppm): 1.38 (9H, $C(CH_3)_3$), 1.71 (3H, CH_3CH), 4.31 (1H, CH_3CH), 4.72 (2H, CO_2CH_2), 5.71 and 6.17 (1H, CH_2=C). ^{13}C NMR: δ (ppm): 21.5 (CH_3CH), 27.9 ($C(CH_3)_3$), 39.6 (CH_3CH), 63.6 (CO_2CH_2), 81.3 ($C(CH_3)_3$), 126.5 (CH_2=C), 136.1 (CH_2=C), 163.9 ($CO_2C(CH_3)_3$), 169.4 (CO_2CH_2).

RAFT Homopolymerization of Acrylic Monomer. AIBN (0.082 g, 0.50 mmol) and CDB (0.408 g, 1.50 mmol) were first added to a 25 mL Schlenk flask (flame-dried under vacuum prior to use) sealed with a rubber septum for degassing and kept under N_2. Next, *t*BBPMA **1** (11.00 g, 37.52 mmol) and dry toluene (3.0 mL) were charged via a gastight syringe. The flask was degassed by three cycles of freezing−pumping−thawing followed by immersing the flask into an oil bath set at 70 °C. The polymerization was terminated by immersing the flask into liquid N_2 after 12 h. THF was added to dilute the solution, and the solution was precipitated into hexane. After repeated purification by dissolving in THF and precipitating in hexane, 4.75 g of pink powder was obtained after drying *in vacuo*. AIBN was used to remove the dithiobenzoate moiety according to previous report.[53] Finally, a white powder, poly(*tert*-butyl 2-((2-bromopropanoyloxy)methyl)acrylate) (P*t*BBPMA) **2**, was obtained after drying *in vacuo*. GPC: M_n = 6200, M_w/M_n = 1.06. FT-IR: ν (cm^{-1}): 2978, 2932, 1736, 1448, 1394, 1368, 1253, 1143, 998, 970, 842, 753. ^1H NMR: δ (ppm): 1.45 (9H, $C(CH_3)_3$), 1.86 (2H, CH_2CCO_2 and 3H, CH_3CH), 4.53 (1H, CH_3CH and 2H, CO_2CH_2). ^{13}C NMR: δ (ppm): 21.9 (CH_3CH), 28.2 ($C(CH_3)_3$), 40.5 (CH_2CCO_2 and CH_3CH), 49.4 (CH_2CCO_2), 65.6 (CO_2CH_2), 83.2 ($C(CH_3)_3$), 169.5 (CO_2CH_2), 171.5 ($CO_2C(CH_3)_3$). Element analysis: Br% = 27.12%.

Functionalization of PPO. In a typical procedure, PPO-OH (10.00 g, M_n = 1000, 10 mmol), succinic anhydride (2.5018 g, 25 mmol), DMAP (0.1222 g, 1 mmol), and dry chloroform (250 mL) were added to a 500 mL three-neck flask, and the mixture was stirred at 80 °C for 18 h. Chloroform was removed by rotary evaporation, and unreacted succinic anhydride was eliminated by filtration. The filtrate was diluted with chloroform and washed with brine. A yellowish liquid, carboxyl-functionalized PPO (PPO-COOH, 7.76 g, 70.5%) was obtained by silica column chromatography. FT-IR: ν (cm^{-1}): 3489 (COOH), 2971, 2870, 1736 (C=O), 1459, 1374, 1345, 1297, 1112, 1014, 928, 866.

PPO-COOH (3.8315 g, 3.48 mmol) and thionyl chloride (20 mL, 275.4 mmol) were added to a 50 mL flask, and the mixture was stirred at room temperature for 2.5 h. Unreacted thionyl chloride was removed *in vacuo* at 50 °C to obtain acyl-chloride-functionalized PPO (PPO-COCl). Next, HTEMPO (2.1750 g, 13.92 mmol), DMAP (0.0510 g, 0.4176 mmol), TEA (0.5 mL, 3.48 mmol), and dry THF (60 mL) were added to a 250 mL three-neck flask, and the solution was cooled to 0 °C for adding PPO-COCl (dissolved in 60 mL of dry THF). The system was stirred at 0 °C for 1 h and was raised to room temperature with further stirring for 1 day. Brine was added to terminate the reaction. The organic phase was washed with water until the aqueous layer turned colorless. After drying over anhydrous $MgSO_4$, an orange liquid, TEMPO-functionalized PPO (PPO-TEMPO) **3a** (2.846 g, 65.1%), was obtained by silica column chromatography. MAIDI-TOF-MS (*m*/*z*): found M^+: 1317. FT-IR: ν (cm^{-1}): 2971, 2870, 1737 (C=O), 1458, 1374, 1345, 1297, 1259, 1111, 1014, 929, 868. ^1H NMR (CD_3OD in the presence of Pd/C and $HCOONH_4$): δ (ppm): 0.92 (3H, $OCH_2CH_2CH_2CH_3$), 1.12 (3H, OCH_2CHCH_3 and 12H, CH_3 of TEMPO), 1.46 (4H, $OCH_2CH_2CH_2CH_3$), 1.84 (4H, CH_2 of TEMPO), 2.57 (4H, $CO_2CH_2CH_2CO_2$), 3.49 (1H, OCH_2CHCH_3), 3.60 (2H, OCH_2CHCH_3 and 2H, $OCH_2CH_2CH_2CH_3$).

ATNRC between P*t*BBPMA and PPO-TEMPO Catalyzed by CuBr/PMDETA. In a typical procedure, CuBr (0.0286 g, 0.1991 mmol) and P*t*BBPMA **2** (0.0587 g, M_n = 6200, M_w/M_n = 1.06, Br % = 27.12%) were added to a 50 mL Schlenk flask (flame-dried under vacuum prior to use) sealed with a rubber septum under N_2. After three cycles of evacuating and purging with N_2, PPO-TEMPO **3a** (0.3000 g, 0.2389 mmol) in 10 mL of dry toluene and PMDETA (0.042 mL, 0.1991 mmol) were charged via a gastight syringe. The flask was degassed by three cycles of freezing−pumping−thawing followed by stirring at room temperature for 10 min. Next, the flask was immersed into an oil bath set at 90 °C. The coupling reaction lasted 1 day, and it was terminated by putting the flask into liquid N_2. The reaction mixture was diluted with THF and passed through a neutral alumina column to remove the residual copper complex. The purification of raw product was performed by dissolving in CH_3OH and filtering through an ultrafiltration membrane separator. The remaining CH_3OH solution in the separator was concentrated and dried *in vacuo* overnight to obtain P*t*BA-*g*-PPO **4c** graft copolymer. GPC: M_n = 25 800, M_w/M_n = 1.05. FT-IR: ν (cm^{-1}): 2974, 2933, 1736, 1458, 1370, 1343, 1253, 1149, 925, 842, 749. ^1H NMR: δ (ppm): 0.91 (3H, $OCH_2CH_2CH_2CH_3$), 1.14 (3H, OCH_2CHCH_3 and 12H, CH_3 of TEMPO), 1.47 (9H, $O(CH_3)_3$ and 4H, $OCH_2CH_2CH_2CH_3$), 1.81 (3H, CH_3CHBr, 2H, CH_2CCO_2 and 4H, CH_2 of TEMPO),

2.60 (4H, $CO_2CH_2CH_2CO_2$), 3.43 (1H, OCH_2CHCH_3), 3.56 (2H, OCH_2CHCH_3 and 2H, $OCH_2CH_2CH_2CH_3$), 4.51 (1H, CH_3CHBr and 2H, CO_2CH_2), 5.03 (1H, CH of TEMPO). ^{13}C NMR: δ (ppm): 14.1 ($OCH_2CH_2CH_2CH_3$), 17.5 (OCH_2CHCH_3), 19.5 ($OCH_2CH_2CH_2CH_3$), 21.3 ($NCCH_3$), 22.0 (CH_3CH), 28.3 ($C(CH_3)_3$), 29.4 ($CO_2CH_2CH_2CO_2$), 31.9 ($OCH_2CH_2CH_2CH_3$), 33.8 ($CO_2CH(CH_2)_2$), 40.6 (CH_2CCO_2 and CH_3CHBr), 44.6 ($NCCH_3$), 49.4 (CH_2CCO_2), 60.4 (CO_2CH_2), 70.5 ($CO_2CH(CH_2)_2$), 71.4 ($OCH_2CH_2CH_2CH_3$), 71.9 (CH_3CHON), 73.5 (OCH_2CHCH_3), 75.5 (OCH_2CHCH_3), 83.3 ($C(CH_3)_3$), 169.7 (CO_2CH_2), 172.0 ($CO_2C(CH_3)_3$ and $CO_2CH_2CH_2CO_2$).

ATNRC between P*t*BBPMA and PPO-TEMPO Catalyzed by Cu/PMDETA. Cu powder (0.0126 g, 0.1991 mmol) and P*t*BBPMA **2** (0.0587 g, M_n = 6200, M_w/M_n = 1.06, Br% = 27.12%) were added to a 50 mL Schlenk flask (flame-dried under vacuum prior to use) sealed with a rubber septum under N_2. After three cycles of evacuating and purging with N_2, PPO-TEMPO **3a** (0.3000 g, 0.2389 mmol) in 10 mL of dry toluene and PMDETA (0.042 mL, 0.1991 mmol) were charged via a gastight syringe. The flask was degassed by three cycles of freezing−pumping− thawing followed by stirring at 20 °C for 2 days, and it was terminated by putting the flask into liquid N_2. The reaction mixture was diluted with THF and passed through a neutral alumina column to remove the residual copper complex. The purification of raw product was performed by dissolving in CH_3OH and filtering through an ultrafiltration membrane separator. The remaining CH_3OH solution in the separator was concentrated and dried *in vacuo* overnight to obtain P*t*BA-*g*-PPO **4d** graft copolymer. GPC: M_n = 25 300, M_w/M_n = 1.05.

Selective Acidic Hydrolysis of P*t*BA-*g*-PPO. P*t*BA-*g*-PPO **4** was dissolved in CH_2Cl_2 and treated with excess trifluoroacetic acid (10-fold) at 40 °C for 32 h. The solution was concentrated and precipitated into cold hexane. After filtration, PAA-*g*-PPO **5** amphiphilic graft copolymer was obtained after drying *in vacuo* overnight. FT-IR: ν (cm^{-1}): 3445 (COOH), 2973, 2933, 2584, 1736, 1449, 1376, 1236, 1158, 1104, 1007, 832, 758. ^1H NMR: δ (ppm): 0.91 (3H, $OCH_2CH_2CH_2CH_3$), 1.14 (3H, OCH_2CHCH_3 and 12H, CH_3 of TEMPO), 1.54 (4H, $OCH_2CH_2CH_2CH_3$), 1.82 (3H, CH_3CHBr, 2H, CH_2CCO_2 and 4H, CH_2 of TEMPO), 2.59 (4H, $CO_2CH_2CH_2CO_2$), 3.43 (1H, OCH_2CHCH_3), 3.56 (2H, OCH_2CHCH_3 and 2H, $OCH_2CH_2CH_2CH_3$), 4.50 (1H, CH_3CHBr and 2H, CO_2CH_2), 5.03 (1H, CH of TEMPO). ^{13}C NMR: δ (ppm): 14.1 ($OCH_2CH_2CH_2CH_3$), 17.5 (OCH_2CHCH_3), 19.5 ($OCH_2CH_2CH_2CH_3$), 21.2 ($NCCH_3$), 22.9 (CH_3CH), 29.9 ($CO_2CH_2CH_2CO_2$), 32.0 ($OCH_2CH_2CH_2CH_3$), 33.7 ($CO_2CH(CH_2)_2$), 40.5 (CH_2CCO_2 and CH_3CHBr), 44.3 ($NCCH_3$), 47.8 (CH_2CCO_2), 60.6 (CO_2CH_2), 70.5 ($CO_2CH(CH_2)_2$), 71.4 ($OCH_2CH_2CH_2CH_3$), 71.9 (CH_3CHON), 73.5 (OCH_2CHCH_3), 75.5 (OCH_2CHCH_3), 169.7 (CO_2CH_2), 172.1 ($CO_2CH_2CH_2CO_2$), 179.7 (COOH).

Determination of Critical Micelle Concentration. Pyrene was used as fluorescence probe to measure the critical micelle concentration (cmc) of PAA-*g*-PPO **5** amphiphilic graft copolymer. Acetone solution of pyrene (0.1286 mM) was added to a large amount of water until the concentration of pyrene reached 0.0006 mM. Different amounts of THF solutions of PAA-*g*-PPO **5** (10, 1, 0.1, 0.01, 0.001, or 0.0001 mg/mL) were added to pyrene-containing water ([pyrene] = 0.0006 mM).

Results and Discussion

Synthesis of Br-Containing Acrylic Monomer. The key intermediate, *tert*-butyl (2-hydroxymethyl)acrylate, was first prepared via Baylis−Hillman reaction using *tert*-butyl acrylate as starting material under base-catalyzed and water-promoted conditions. DABCO and TEA were used as basic cocatalysts, and a protonic solvent H_2O was employed to accelerate the reaction through either the stabilization of enolate or the activation of aldehyde.[54,55] Next, 2-bromopropionic acid reacted with *tert*-butyl (2-hydroxymethyl)-acrylate to provide the desired Br-containing *t*BBPMA **1** monomer via the common esterification using DMAP as catalyst.

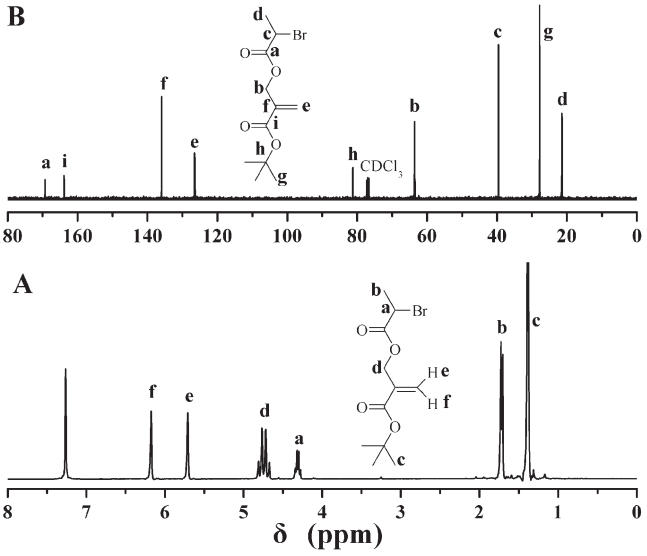

Figure 1. ^1H NMR (A) and ^{13}C NMR (B) spectra of *t*BBPMA **1** in $CDCl_3$.

FT-IR, ^1H NMR, and ^{13}C NMR were used to characterize the chemical structure of *t*BBPMA **1**. Typical signals of carbonyl and double bond appeared at 1748, 1720, and 1643 cm^{-1} in the FT-IR spectrum. The resonance signals of double bond were found to locate at 5.71 and 6.17 ppm in the ^1H NMR spectrum (Figure 1A). The peaks at 4.31 and 4.72 ppm belonged to 1 proton of $CHBr$ and 2 protons of CO_2CH_2, respectively. The typical peaks at 126.5, 136.1, 163.9, and 169.4 ppm in the ^{13}C NMR spectrum (Figure 1B) also witnessed the presence of double bond and carbonyl. All these evidence demonstrated the successful synthesis of Br-containing acrylic monomer *t*BBPMA **1**.

Preparation of Well-Defined P*t*BA-Based Backbone. *t*BBPMA **1** was homopolymerized via RAFT in toluene using AIBN as initiator and CDB as chain transfer agent. AIBN was employed to remove the moiety of dithiobenzoate end group according to previous literature.[53] The pink powder turned into white powder after the reaction, indicating the absence of dithiobenzoate residue.

The FT-IR spectrum showed the disappearance of typical signal of double bond at 1643 cm^{-1} after RAFT homopolymerization. The peak of polyacrylate backbone appeared at 1.86 ppm in the ^1H NMR spectrum after the homopolymerization (Figure 2A) whereas the resonance signals of the double bond disappeared. In particular, the resonance signal of 1 proton of $CHBr$ was found to locate at 4.53 ppm, and the bromine content after the homopolymerization (27.12%) was almost the same as that of the monomer (27.20%), which showed that the $CHBr$ group was not affected during the homopolymerization. The disappearance of the resonance signals of the double bond was also verified by the ^{13}C NMR spectrum (Figure 2B), and the peak of carbonyl of $CO_2C(CH_3)_3$ shifted from 163.9 to 171.5 ppm after RAFT homopolymerization.

In addition, only a unimodal and symmetrical elution peak with narrow molecular weight distribution (M_w/M_n = 1.06) was found in the GPC curve (Figure 3) after RAFT homopolymerization of *t*BBPMA **1**. From the data of molecular weight (M_n = 6200), we can estimate that every

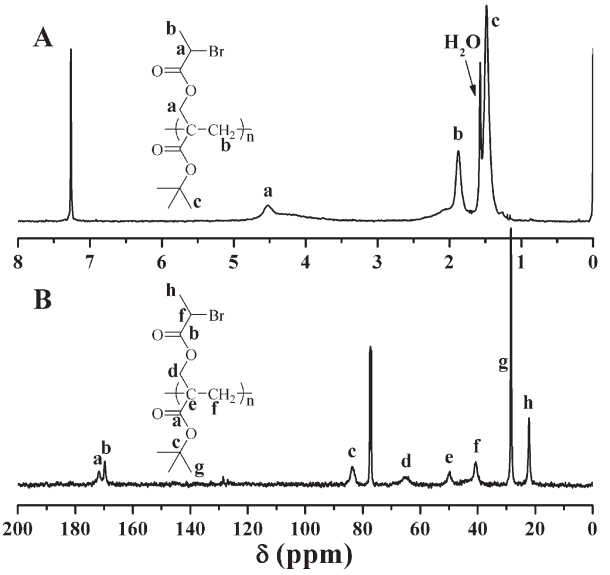

Figure 2. ^{1}H NMR (A) and ^{13}C NMR (B) spectra of P*t*BBPMA **2** in $CDCl_3$.

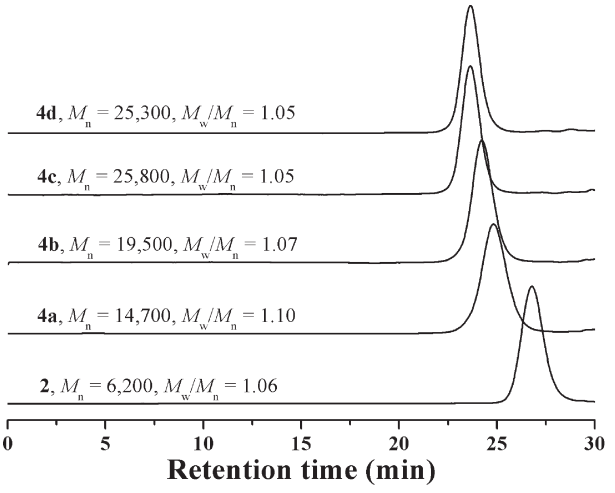

Figure 3. GPC traces of P*t*BBPMA **2** and P*t*BA-*g*-PPO **4a**, **4b**, **4c**, and **4d** in THF.

P*t*BBPMA **2** chain possesses 20.5 repeating units. All the above results confirmed the formation of well-defined P*t*BA-based backbone.

Preparation of TEMPO-Functionalized PPO. PPO-OH was first esterified by succinic anhydride to provide PPO-COOH. The successful introduction of carboxyl group was evidenced by two new peaks at 3489 and 1736 cm^{-1} in the FT-IR spectrum after the reaction. Next, PPO-COOH was almost quantitatively converted to PPO-COCl by reacting with $SOCl_2$ followed by adding HTEMPO *in situ* to obtain the orange PPO-TEMPO compared to the colorless PPO-OH. A typical signal of CH_2 of TEMPO located at 1.84 ppm in the ^{1}H NMR spectrum after the reaction, confirming the existence of TEMPO radical. The peaks of CH_3 and CH of TEMPO were overlapped with those of PPO and CD_3OD, respectively. In addition, the peak at 2.57 ppm is attributed to 4 protons of $CO_2CH_2CH_2CO_2$ connection between TEMPO end group and PPO segment, which also illustrated the successful incorporation of TEMPO radical. The molecular weight of the product derived from PPO-OH (M_n = 1000 g/mol) is 1317 g/mol (Table 1) measured by MAIDI-TOF-MS, which is in good accordance with the theoretical value (1254 g/mol). All these points demonstrated the successful preparation of functionalized PPO with TEMPO end group. The approximate number of PO repeating unit per chain (N_{PPO}) can be calculated from the molecular weight of PPO-OH, and the values are 16.0 and 41.9 for PPO-TEMPO **3a** and **3b**, respectively.

Table 1. Preparation of TEMPO-Functionalized PPO

sample	M_n[c] (g/mol)	M_n[d] (g/mol)	M_w/M_n[e]	N_{PPO}[f]
3a[a]	1254	1317	1.07	16.0
3b[b]	2754		1.11	41.9

[a] Synthesized from PPO-OH, M_n = 1000. [b] Synthesized from PPO-OH, M_n = 2500. [c] Theoretical molecular weight. [d] Measured by MAIDI-TOF-MS. [e] Measured by GPC in THF. [f] The number of PO repeating unit per chain.

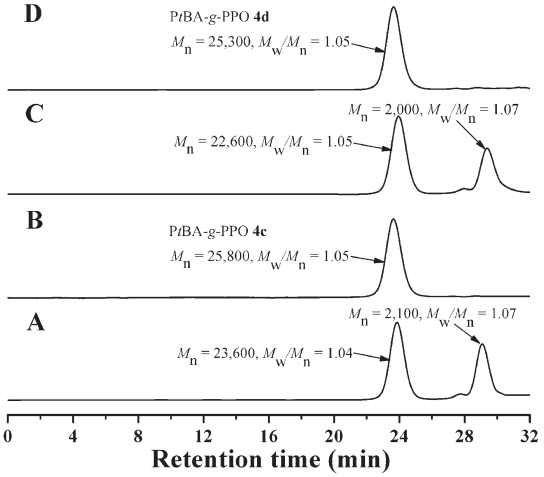

Figure 4. GPC traces of P*t*BA-*g*-PPO **4c** and **4d** before and after the ultrafiltration.

Table 2. Synthesis of P*t*BA-*g*-PPO Graft Copolymer

sample	[**3**]/[Br group]	M_n[d] (g/mol)	M_w/M_n[d]	n_{PPO}[e]	D_{graft}[f] (%)
4a[a]	0.4/1	14 700	1.10	4.0	19.5
4b[a]	0.7/1	19 500	1.07	6.9	33.7
4c[a]	1.2/1	25 800	1.05	11.6	56.6
4d[b]	1.2/1	25 300	1.05	12.0	58.5
4e[c]	0.4/1	35 900	1.17	4.7	22.9
4f[c]	0.7/1	47 500	1.23	8.6	42.0
4g[c]	1.2/1	52 500	1.13	13.4	65.4

[a] Synthesized from PPO-TEMPO **3a** catalyzed by CuBr/PMDETA at 90 °C for 24 h. [b] Synthesized from PPO-TEMPO **3a** catalyzed by Cu/PMDETA at 20 °C for 24 h. [c] Synthesized from PPO-TEMPO **3b** catalyzed by CuBr/PMDETA at 90 °C for 24 h. [d] Measured by GPC in THF at 35 °C. [e] The number of grafted PPO side chain obtained by ^{1}H NMR. [f] The grafting density of PPO side chain.

Synthesis of P*t*BA-*g*-PPO Graft Copolymer via ATNRC. ATNRC reaction between Br-containing P*t*BBPMA **2** homopolymer and PPO-TEMPO **3** was performed in toluene at 90 °C using CuBr/PMDETA as the catalytic system.[47−51] The crude product was a mixture of P*t*BA-*g*-PPO graft copolymer and unreacted PPO-TEMPO as evidenced by GPC (Figure 4A). The mixture was separated by an ultrafiltration membrane separator to provide pure P*t*BA-*g*-PPO **4** graft copolymer as shown in Figure 4B. It is clear that all the molecular weights of the obtained graft copolymers are much higher than that of P*t*BBPMA **2** homopolymer as listed in Table 2, indicating the occurring of the coupling reaction. All graft copolymers' GPC curves (Figure 3) showed a unimodal and symmetrical elution peak with narrow molecular weight distribution ($M_w/M_n \leq 1.23$), and the molecular weights increased with the raising of the composition of PPO-TEMPO **3** in the feed ratios.

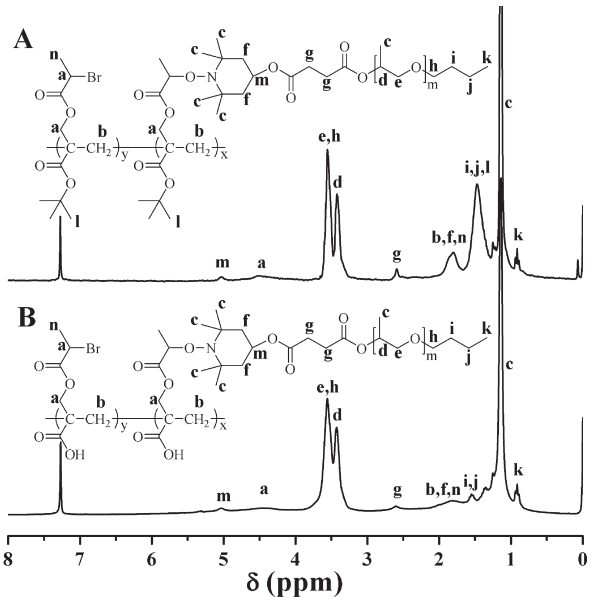

Figure 5. ^{1}H NMR spectra of P*t*BA-*g*-PPO **4** (A) and PAA-*g*-PPO **5** (B) in $CDCl_3$.

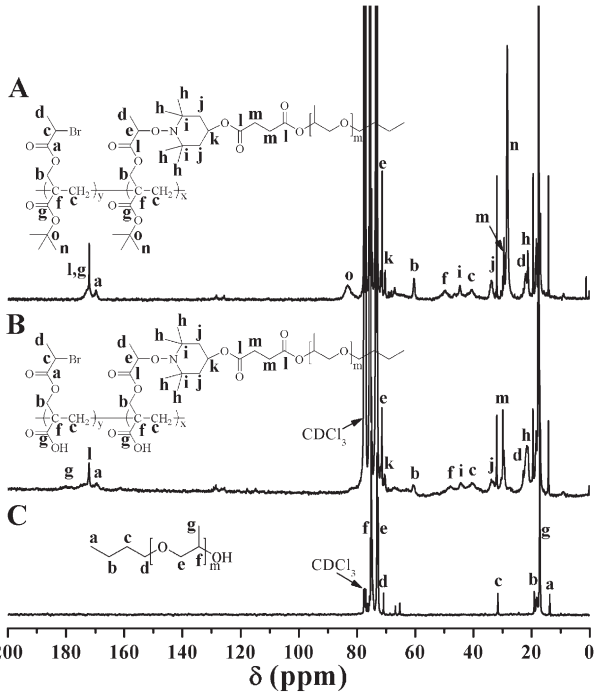

Figure 6. ^{13}C NMR spectra of P*t*BA-*g*-PPO **4** (A), PAA-*g*-PPO **5** (B), and PPO-OH (C) in $CDCl_3$.

The resonance signals of the corresponding protons of both P*t*BA backbone and PPO side chains are found in the ^{1}H NMR spectrum as shown in Figure 5A. The peaks at 1.14 (OCH_2CHCH_3), 3.43 (OCH_2CHCH_3), and 3.56 ppm (OCH_2CHCH_3) are attributed to PPO side chains. A typical signal of 9 protons of *tert*-butyl of P*t*BA backbone locates at 1.47 ppm, which is overlapped with the signal of 4 protons of $OCH_2CH_2CH_2CH_3$ end group of PPO side chains. The minor peak at 5.03 ppm (peak "m") belongs to 1 proton of C*H* of piperidine, which demonstrated the existence of TEMPO linkage between P*t*BA backbone and PPO side chains.

Figure 6A shows the ^{13}C NMR spectrum of P*t*BA-*g*-PPO **4**. The peaks at 14.1 ($OCH_2CH_2CH_2CH_3$), 17.5 (OCH_2CHCH_3), 19.5 ($OCH_2CH_2CH_2CH_3$), 31.9 ($OCH_2CH_2CH_2CH_3$), 71.4 ($OCH_2CH_2CH_2CH_3$), 73.5 (OCH_2CHCH_3), and 75.5 ppm (OCH_2CHCH_3) are attributed to PPO side chains compared to ^{13}C NMR spectrum of PPO-OH (Figure 6C). Typical signals of *tert*-butyl of P*t*BA backbone are found to locate at 28.3 ($C(CH_3)_3$) and 83.3 ppm ($C(CH_3)_3$). The TEMPO connection between P*t*BA backbone and PPO side chains is also evidenced by the peaks at 21.3 ($NCCH_3$), 33.8 ($CO_2CH(CH_2)_2$), 44.6 ($NCCH_3$), and 70.5 ppm ($CO_2CH(CH_2)_2$).

Scheme 2. Mechanism of Cu^0-Catalyzed ATNRC Reaction

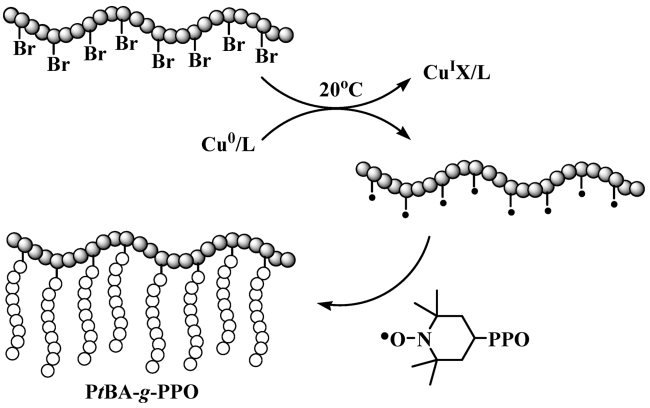

Generally, ATNRC reaction was catalyzed by a relatively expensive catalyst, CuBr (Aldrich 212865, 98%, US $70.90/250 g), under a relatively high temperature (90 °C), which may cause some side reactions including the chain transfer and the cross-linking. Is it possible to optimize ATNRC so that it can be run under the relatively mild conditions? Percec and co-workers have developed SET-LRP,[37,38] in which Cu^0 powder (Aldrich 207780, 99%, US $41.60/500 g) was used as an economical catalyst instead of Cu^I at ambient temperature.[56−67] Thus, it is feasible to adopt Cu^0 powder instead of CuBr to generate the macroradicals according to the mechanism of SET-LRP to synthesize P*t*BA-*g*-PPO graft copolymer under the relatively mild conditions. This experiment was carried out in toluene at 20 °C using the Cu^0/PMDETA catalytic system, and a well-defined P*t*BA-*g*-PPO graft copolymer **4d** (M_n = 25 300, M_w/M_n = 1.05) was successfully synthesized with a similar grafting density (Table 2) and GPC curve (Figure 4D) in comparison with the entry of **4c** catalyzed by CuBr/PMDETA at 90 °C (Table 2). This strategy is similar to SET-NRC recently reported by Huang and co-workers,[68] in which THF and ethanol were as solvents. In the current system, equimolar Cu^0 transferred an electron to Br-containing repeating unit (P-Br) to afford the macroradical and Cu^I by the SET mechanism,[37,38,56−67] as shown in Scheme 2. The formed macroradicals were captured by TEMPO-functionalized PPO so that PPO side chains were linked to the backbone.

Since the molecular weight of graft copolymer measured by GPC is very different from the "real" value,[69] the number of grafted PPO side chains (n_{PPO}) was determined by ^{1}H NMR instead of GPC. This value was calculated according to eq 1 (*S* is the peak area, and N_{PPO} (16.0 or 41.9) is the number of PO repeating unit per side chain) as listed in Table 2. Furthermore, the grafting density of PPO side chain (D_{graft}) was calculated via eq 2 (20.5 is the number of *t*BA repeating unit of the backbone), and the results are summarized in Table 2. Thus, the grafting efficiency can be estimated to be in the range from 48% to 65%, which is similar to that of a recent report about synthesizing the graft copolymers via ATNRC strategy.[48] Another recent article also reported the moderate coupling efficiency (36−75%) of the Cu^I-catalyzed click "grafting-onto" reaction.[70] Relatively low efficiency is

typical in synthesizing the graft copolymer via the grafting-onto strategy due to the steric hindrance of the dense structure of the graft copolymer.[48,70] From the above results, it can be concluded that the synthesized graft copolymers, P*t*BA-*g*-PPO **4**, possess well-defined structure: a poly(*tert*-butyl acrylate) backbone (20.5 repeating units) and 4.0−13.4 grafted PPO side chains with certain length (16.0 or 41.9 repeating units per side chain).

$$S_{d,e,h}/S_{i,j,1} = (3N_{PPO}+2)n_{PPO}/(20.5\times 9+4n_{PPO}) \quad (1)$$

$$D_{graft} = n_{PPO}/20.5 \quad (2)$$

Selective Hydrolysis of P*t*BA Backbone. Trifluoroacetic acid was used to hydrolyze the hydrophobic P*t*BA backbone to the hydrophilic PAA backbone in CH_2Cl_2 according to previous literatures.[71−73] The chemical structure of the hydrolyzed product was characterized by ^{1}H NMR, ^{13}C NMR, and FT-IR. The integration area of the peak at 1.47 ppm in the ^{1}H NMR spectrum after the hydrolysis (Figure 5B) reduced remarkably due to the disappearance of the signal of 9 protons of *tert*-butyl group. Moreover, the characteristic signals of the carbons of $C(CH_3)_3$ group at 28.3 (peak "n" in Figure 6A) and 83.3 (peak "o" in Figure 6A) ppm in the ^{13}C NMR spectrum completely disappeared after the hydrolysis as shown in Figure 6B, which demonstrated the successful hydrolysis of P*t*BA backbone. A new broad peak of −COOH appeared at 3445 cm^{-1} in the FT-IR spectrum after the hydrolysis (Figure 7A) in comparison with that before the hydrolysis (Figure 7B), indicating the presence of carboxyl groups and the formation of PAA backbone. The minor peak at 5.03 ppm (peak "m") still appeared in Figure 5B after the hydrolysis, which verified the remaining of TEMPO linkage between PAA backbone and PPO side chains. Furthermore, typical signals of PPO side chains remained in both ^{1}H NMR and ^{13}C NMR spectra after the hydrolysis; this confirmed that PPO side chains were not affected during the hydrolysis. Therefore, we can conclude that P*t*BA-*g*-PPO was selectively hydrolyzed to PAA-*g*-PPO.

Self-Assembly of PAA-*g*-PPO Amphiphilic Graft Copolymer. The cmc values of PAA-*g*-PPO **5** amphiphilic graft copolymers in aqueous media were examined by the fluorescence technique using pyrene as probe.[74,75] The fluorescence spectrum of pyrene is sensitively influenced by the environment and the polarity of its surrounding.[69,71] In the presence of micelles, pyrene is solubilized within the interior of the hydrophobic part. As a result, the values of I_1/I_3 of the emission spectrum changed sharply. The intensity ratios (I_1/I_3) against the logarithm of polymer concentrations were plotted to determine cmc as the onset of micellization (Figure 8).

The cmc values of PAA-*g*-PPO **5** are summarized in Table 3. These values were comparable with those of polymeric amphiphiles.[76−79] The cmc values of PAA-*g*-PPO decreased when the molecular weights increased due to the increasing of the content of hydrophobic PPO side chains.

As for PPO-based amphiphilic copolymers, only a few examples touched on their self-assembly properties in the selective solvents. Liu and co-workers reported the reversible temperature-induced self-assembly process of PPO-based block copolymers.[5,6] Furthermore, the sizes and morphologies of PEO-*b*-PPO amphiphilic diblock copolymer changed as the variation of the concentration of the aqueous solution.[19] However, none has reported the micellar morphology of PPO-based amphiphilic graft copolymer. The studies on the micellar morphology of PAA-*g*-PPO amphiphilic graft copolymer may make sense. Eisenberg and co-workers found that the micellar morphologies formed by PS-*b*-PAA amphiphilic diblock copolymers could be tuned by the compositions of the copolymers.[80] Thus, it may be interesting to investigate the micellar morphology of PAA-*g*-PPO **5** amphiphilic graft copolymer with the changing of the content of hydrophobic PPO segment.

In the current work, micellar structures were investigated by TEM. Diverse morphologies, including spheres, branched short rods, nanofibers, and vesicles, were formed by PAA-*g*-PPO **5** graft copolymers with different molecular weights in pure water (Figure 9). Figure 9A shows the spherical micelles (ca. 340 nm) formed by PAA-*g*-PPO **5a** synthesized from PPO-TEMPO **3a**. These spherical micelles

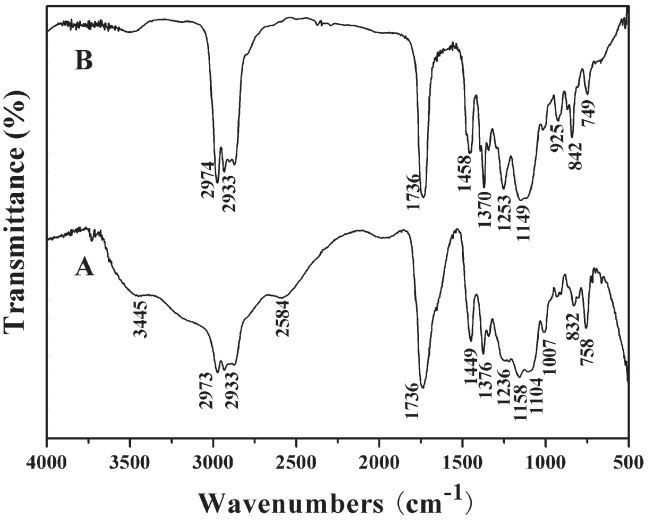

Figure 7. FT-IR spectra of PAA-*g*-PPO **5** (A) and P*t*BA-*g*-PPO **4** (B).

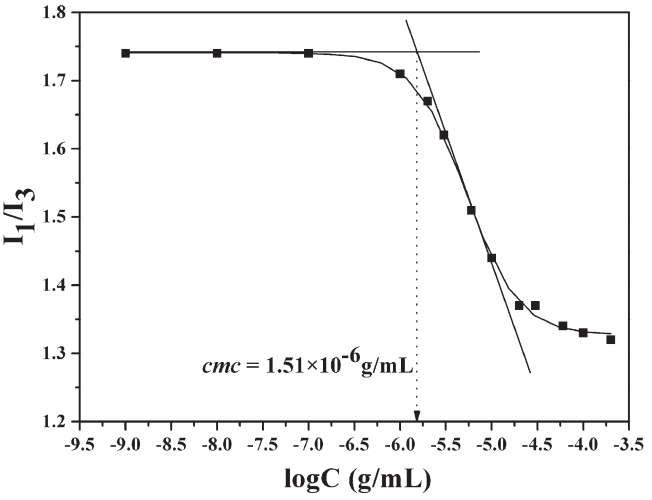

Figure 8. Dependence of fluorescence intensity ratios of pyrene emission bands on the concentrations of PAA-*g*-PPO **5b**.

Table 3. cmc of PAA-*g*-PPO Amphiphilic Graft Copolymer[a]

P*t*BA-*g*-PPO	PAA-*g*-PPO	cmc (g/mL)
4a	**5a**	2.08×10^{-6}
4b	**5b**	1.51×10^{-6}
4c	**5c**	9.57×10^{-7}
4e	**5e**	1.47×10^{-6}
4f	**5f**	1.24×10^{-6}
4g	**5g**	9.84×10^{-7}

[a] Determined by fluorescence spectroscopy using pyrene as probe.

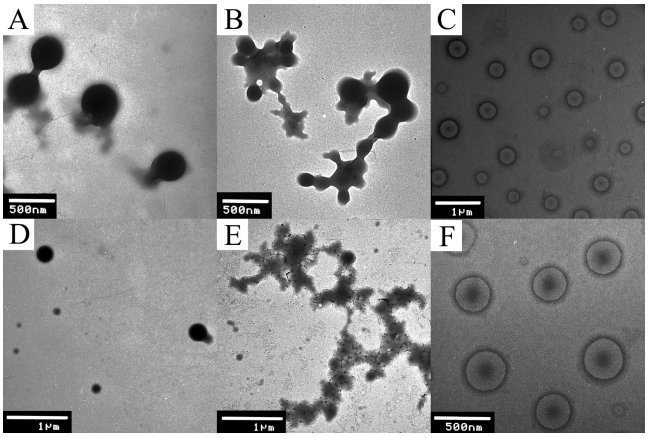

Figure 9. TEM images of micelles formed by PAA-*g*-PPO **5a** (A), **5b** (B), **5c** (C), **5e** (D), **5f** (E), and **5g** (F) in pure water.

have a trend to link into rod structures. When the grafting density of PPO-TEMPO **3a** increased to 33.7%, the micellar morphologies of PAA-*g*-PPO **5b** were branched short rods (Figure 9B). On further increasing the grafting density of PPO-TEMPO **3a** to 56.6%, PAA-*g*-PPO **5c** aggregated to form vesicles (ca. 500 nm) as shown in Figure 9C. PAA-*g*-PPO **5e**, **5f**, and **5g** synthesized from PPO-TEMPO **3b** also have a similar trend. With the increasing of the grafting density of PPO-TEMPO **3b**, spherical micelles (ca. 270 nm) formed by PAA-*g*-PPO **5e** (Figure 9D) changed into nanofibers (Figure 9E) aggregated by PAA-*g*-PPO **5f** containing more PPO segments. PAA-*g*-PPO **5g** with the highest grafting density (65.4%) aggregated into vesicles (ca. 420 nm), as shown in Figure 9F. This phenomena is similar to previous report.[80] From a thermodynamic point of view, an increase of the aggregation number which decreases the interface area between the solvent and the aggregating blocks is favored. For the case of the spheres, along with the rising of the content of hydrophobic PPO segments, the aggregation number increases and the core radius also has to increase. As a result, the degree of stretching of PPO chains has to increase correspondingly, which is thermodynamically unfavorable. However, for the rod structures, the additional freedom degree along the axis made many chains incorporate into the structure without remarkable changes in their original conformation. The same applies to the vesicles. Thus, spherical aggregates transformed into branched micelles and finally into vesicles while the grafting density of hydrophobic PPO side chains increased. Thus, it is clear that the content of hydrophobic PPO segments really played an important role in determining the micellar morphologies.

Conclusions

In summary, we have presented the first example of well-defined PAA-*g*-PPO amphiphilic graft copolymer with narrow molecular weight distribution ($M_w/M_n \leq 1.23$) by sequential reversible addition−fragmentation chain transfer (RAFT) polymerization and atom transfer nitroxide radical coupling (ATNRC) chemistry followed by the selective hydrolysis of poly(*tert*-butyl acrylate) backbone. The molecular weights of the backbone and side chains are both clear. The cmc of the amphiphilic graft copolymer in water was determined by the fluorescence spectroscopy using pyrene as probe and the values decreased with the increasing of the contents of hydrophobic PPO side chains. Diverse micellar morphologies formed by PAA-*g*-PPO are sensitive to the content of hydrophobic PPO segment. These aggregates may provide templates to fabricate nanocomposites, which is being carried out in our group.

Acknowledgment. The authors thank the financial support from National Natural Science Foundation of China (20974117, 20904065, and 50873029), Shanghai Rising Star Program (07QA14066), Shanghai Nano-Technology Program (0952 nm05800), Shanghai Scientific and Technological Innovation Project (08431902300), and Knowledge Innovation Program of the Chinese Academy of Sciences.

References and Notes

(1) Alexandridis, P.; Holzwarth, J. F.; Hatton, T. A. *Macromolecules* **1994**, *27*, 2414–2425.
(2) Alexandridis, P.; Hatton, T. A. *Colloids Surf., A* **1995**, *96*, 1–46.
(3) O'Sickey, M. J.; Lawrey, B. D.; Wilkes, G. L. *J. Appl. Polym. Sci.* **2002**, *84*, 229–243.
(4) Wanka, G.; Hoffmann, H.; Ulbricht, W. *Macromolecules* **1994**, *27*, 4145–4159.
(5) Liu, S. Y.; Billingham, N. C.; Armes, S. P. *Angew. Chem., Int. Ed.* **2001**, *40*, 2328–2331.
(6) Liu, S. Y.; Armes, S. P. *J. Am. Chem. Soc.* **2001**, *123*, 9910–9911.
(7) Lee, M.; Cho, B. K.; Ihn, K. J.; Lee, W. K.; Oh, N. K.; Zin, W. C. *J. Am. Chem. Soc.* **2001**, *123*, 4647–4648.
(8) Anderson, B. C.; Cox, S. M.; Bloom, P. D.; Sheares, V. V.; Mallapragada, S. K. *Macromolecules* **2003**, *36*, 1670–1676.
(9) Ryu, J. H.; Oh, N. K.; Zin, W. C.; Lee, M. *J. Am. Chem. Soc.* **2004**, *126*, 3551–3558.
(10) Barreiro-Iglesias, R.; Bromberg, L.; Temchenko, M.; Hatton, T. A.; Concheiro, A.; Alvarez-Lorenzo, C. *J. Controlled Release* **2004**, *97*, 537–549.
(11) Bromberg, L.; Deshmukh, S.; Temchenko, M.; Iourtchenko, L.; Alakhov, V.; Alvarez-Lorenzo, C.; Barreiro-Iglesias, R.; Concheiro, A.; Hatton, T. A. *Bioconjugate Chem.* **2005**, *16*, 626–633.
(12) Aubrecht, K. B.; Grubbs, R. B. *J. Polym. Sci., Polym. Chem.* **2005**, *43*, 5156–5167.
(13) Li, C. M.; Buurma, N. J.; Haq, I.; Turner, C.; Armes, S. P. *Langmuir* **2005**, *21*, 11026–11033.
(14) Amado, E.; Augsten, C.; Mader, K.; Blume, A.; Kressler, J. *Macromolecules* **2006**, *39*, 9486–9496.
(15) Nair, R. C.; Gopakumar, S.; Nair, M. R. G. *J. Appl. Polym. Sci.* **2007**, *103*, 955–962.
(16) Malik, M. I.; Trathnigg, B.; Kappe, C. O. *Macromol. Chem. Phys.* **2007**, *208*, 2510–2524.
(17) Kyerematen, S. O.; Amado, E.; Blume, A.; Kressler, J. *Macromol. Rapid Commun.* **2008**, *29*, 1140–1146.
(18) Miles, W. C.; Goff, J. D.; Huffstetler, P. P.; Reinholz, C. M.; Pothayee, N.; Caba, B. L.; Boyd, J. S.; Davis, R. M.; Riffle, J. S. *Langmuir* **2009**, *25*, 803–813.
(19) Wang, Y. X.; Tan, Y. B.; Huang, X. L.; Che, Y. J.; Du, X. *J. Appl. Polym. Sci.* **2009**, *112*, 1425–1435.
(20) Maeda, Y.; Tsubota, M.; Ikeda, I. *Macromol. Rapid Commun.* **2003**, *24*, 242–245.
(21) Li, Y. T.; Tang, Y. Q.; Narain, R.; Lewis, A. L.; Armes, S. P. *Langmuir* **2005**, *21*, 9946–9954.
(22) Neugebauer, D. *Polymer* **2007**, *48*, 4966–4973.
(23) Ryu, S. W.; Mayes, A. M. *Polymer* **2008**, *49*, 2268–2273.
(24) Lebedeva, E.; Kesler, B. S.; Carter, K. R. *J. Polym. Sci., Polym. Chem.* **2005**, *43*, 2266–2275.
(25) Block, M. A. B.; Hecht, S. *Macromolecules* **2008**, *41*, 3219–3227.
(26) Mehdipour-Ataei, S.; Saidi, S. *Polym. Adv. Technol.* **2008**, *19*, 889–894.
(27) Portehault, D.; Petit, L.; Pantoustier, N.; Ducouret, G.; Lafuma, F.; Hourdet, D. *Colloids Surf., A* **2006**, *278*, 26–32.
(28) Jannasch, P. *Polymer* **2000**, *41*, 6701–6707.
(29) Zhang, M. F.; Breiner, T.; Mori, H.; Muller, A. H. E. *Polymer* **2003**, *44*, 1449–1458.
(30) Dziezok, P.; Fischer, K.; Schmidt, M.; Sheiko, S. S.; Moller, M. *Angew. Chem., Int. Ed.* **1997**, *36*, 2812–2815.
(31) Heroguez, V.; Gnanou, Y.; Fontanille, M. *Macromolecules* **1997**, *30*, 4791–4798.
(32) Wang, J. S.; Matyjaszewski, K. *J. Am. Chem. Soc.* **1995**, *117*, 5614–5615.
(33) Percec, V.; Barboiu, B. *Macromolecules* **1995**, *28*, 7970–7972.
(34) Kato, M.; Kamigaito, M.; Sawamoto, M.; Higashimura, T. *Macromolecules* **1995**, *28*, 1721–1723.
(35) Moad, G.; Rizzardo, E.; Thang, S. H. *Polymer* **2008**, *49*, 1079–1131.
(36) Moad, G.; Rizzardo, E.; Thang, S. H. *Acc. Chem. Res.* **2008**, *41*, 1133–1142.

(37) Percec, V.; Guliashvili, T.; Ladislaw, J. S.; Wistrand, A.; Stjerndahl, A.; Sienkowska, M. J.; Monteiro, M. J.; Sahoo, S. *J. Am. Chem. Soc.* **2006**, *128*, 14156–14165.
(38) Nguyen, N. H.; Rosen, B. M.; Lligadas, G.; Percec, V. *Macromolecules* **2009**, *42*, 2379–2386.
(39) Beers, K. L.; Gaynor, S. G.; Matyjaszewski, K.; Sheiko, S. S.; Moller, M. *Macromolecules* **1998**, *31*, 9413–9415.
(40) Matyjaszewski, K.; Xia, J. H. *Chem. Rev.* **2001**, *101*, 2921–2990.
(41) Deffieux, A.; Schappacher, M. *Macromolecules* **1999**, *32*, 1797–1802.
(42) Kolb, H. C.; Finn, M. G.; Sharpless, K. B. *Angew. Chem., Int. Ed.* **2001**, *40*, 2004–2021.
(43) Helms, B.; Mynar, J. L.; Hawker, C. J.; Frechet, J. M. J. *J. Am. Chem. Soc.* **2004**, *126*, 15020–15021.
(44) Vestberg, R.; Malkoch, M.; Kade, M.; Wu, P.; Fokin, V. V.; Sharpless, K. B.; Drockenmuller, E.; Hawker, C. J. *J. Polym. Sci., Polym. Chem.* **2007**, *45*, 2835–2846.
(45) Malkoch, M.; Schleicher, K.; Drockenmuller, E.; Hawker, C. J.; Russell, T. P.; Wu, P.; Fokin, V. V. *Macromolecules* **2005**, *38*, 3663–3678.
(46) Lutz, J. F. *Angew. Chem., Int. Ed.* **2007**, *46*, 1018–1025.
(47) Lin, W. C.; Fu, Q.; Zhang, Y.; Huang, J. L. *Macromolecules* **2008**, *41*, 4127–4135.
(48) Fu, Q.; Lin, W. C.; Huang, J. L. *Macromolecules* **2008**, *41*, 2381–2387.
(49) Liu, C.; Pan, M. G.; Zhang, Y.; Huang, J. L. *J. Polym. Sci., Polym. Chem.* **2008**, *46*, 6754–6761.
(50) Fu, Q.; Liu, C.; Lin, W. C.; Huang, J. L. *J. Polym. Sci., Polym. Chem.* **2008**, *46*, 6770–6779.
(51) Fu, Q.; Wang, G. W.; Lin, W. C.; Huang, J. L. *J. Polym. Sci., Polym. Chem.* **2009**, *47*, 986–990.
(52) Moad, G.; Chiefari, J.; Chong, Y. K.; Krstina, J.; Mayadunne, R. T. A.; Postma, A.; Rizzardo, E.; Thang, S. H. *Polym. Int.* **2000**, *49*, 993–1001.
(53) Perrier, S.; Takolpuckdee, P.; Mars, C. A. *Macromolecules* **2005**, *38*, 2033–2036.
(54) Aggarwal, V. K.; Mereu, A.; Tarver, G. J.; McCague, R. *J. Org. Chem.* **1998**, *63*, 7183–7189.
(55) Aggarwal, V. K.; Dean, D. K.; Mereu, A.; Williams, R. *J. Org. Chem.* **2002**, *67*, 510–514.
(56) Percec, V.; Popov, A. V.; Ramirez-Castillo, E.; Monteiro, M.; Barboiu, B.; Weichold, O.; Asandei, A. D.; Mitchell, C. M. *J. Am. Chem. Soc.* **2002**, *124*, 4940–4941.
(57) Percec, V.; Popov, A. V.; Ramirez-Castillo, E.; Weichold, O. *J. Polym. Sci., Polym. Chem.* **2003**, *41*, 3283–3299.
(58) Coelho, J. F. J.; Silva, A. M. F. P.; Popov, A. V.; Percec, V.; Abreu, M. V.; Goncalves, P. M. O. F.; Gil, M. H. *J. Polym. Sci., Polym. Chem.* **2006**, *44*, 3001–3008.
(59) Guliashvili, T.; Percec, V. *J. Polym. Sci., Polym. Chem.* **2007**, *45*, 1607–1618.
(60) Monteiro, M. J.; Guliashvili, T.; Percec, V. *J. Polym. Sci., Polym. Chem.* **2007**, *45*, 1835–1847.
(61) Rosen, B. M.; Percec, V. *J. Polym. Sci., Polym. Chem.* **2007**, *45*, 4950–4964.
(62) Lligadas, G.; Percec, V. *J. Polym. Sci., Polym. Chem.* **2008**, *46*, 2745–2754.
(63) Rosen, B. M.; Percec, V. *J. Polym. Sci., Polym. Chem.* **2008**, *46*, 5663–5697.
(64) Lligadas, G.; Percec, V. *J. Polym. Sci., Polym. Chem.* **2008**, *46*, 6880–6895.
(65) Lligadas, G.; Rosen, B. M.; Monteiro, M. J.; Percec, V. *Macromolecules* **2008**, *41*, 8360–8364.
(66) Lligadas, G.; Rosen, B. M.; Bell, C. A.; Monteiro, M. J.; Percec, V. *Macromolecules* **2008**, *41*, 8365–8371.
(67) Wright, P. M.; Mantovani, G.; Haddleton, D. M. *J. Polym. Sci., Polym. Chem.* **2008**, *46*, 7376–7385.
(68) Fu, Q.; Zhang, Z. N.; Lin, W. C.; Huang, J. L. *Macromolecules* **2009**, *42*, 4381–4383.
(69) Jia, Z. F.; Fu, Q.; Huang, J. L. *Macromolecules* **2006**, *39*, 5190–5193.
(70) Tsarevsky, N. V.; Bencherif, S. A.; Matyjaszewski, K. *Macromolecules* **2007**, *40*, 4439–4445.
(71) O'Reilly, R. K.; Joralemon, M. J.; Wooley, K. L.; Hawker, C. J. *Chem. Mater.* **2005**, *17*, 5976–5988.
(72) Ruehl, J.; Nilsen, A.; Born, S.; Thoniyot, P.; Xu, L. P.; Chen, S. W.; Braslau, R. *Polymer* **2007**, *48*, 2564–2571.
(73) Li, P. P.; Li, Z. Y.; Huang, J. L. *Macromolecules* **2007**, *40*, 491–498.
(74) Wilhelm, M.; Zhao, C. L.; Wang, Y. C.; Xu, R. L.; Winnik, M. A.; Mura, J. L.; Riess, G.; Croucher, M. *Macromolecules* **1991**, *24*, 1033–1040.
(75) Astafieva, I.; Zhong, X.; Eisenberg, A. *Macromolecules* **1993**, *26*, 7339–7352.
(76) Zhang, L. F.; Yu, K.; Eisenberg, A. *Science* **1996**, *272*, 1777–1779.
(77) Yagci, Y.; Atilla Tasdelen, M. *Prog. Polym. Sci.* **2006**, *31*, 1133–1170.
(78) Muhlebach, A.; Gaynor, S. G.; Matyjaszewski, K. *Macromolecules* **1998**, *31*, 6046–6052.
(79) Clendenning, S. B.; Fournier-Bidoz, S.; Pietrangelo, A.; Yang, G. C.; Han, S. J.; Brodersen, P. M.; Yip, C. M.; Lu, Z. H.; Ozin, G. A.; Manners, I. *J. Mater. Chem.* **2004**, *14*, 1686–1690.
(80) Zhang, L. F.; Eisenberg, A. *J. Am. Chem. Soc.* **1996**, *118*, 3168–3181.